Mon. Not. R. astr. Soc. (1978) **185**, 109–122

Predictions and strategies for deep X-ray surveys

A. C. Fabian and M. J. Rees *Institute of Astronomy, Madingley Road, Cambridge CB3 0HA*

Received 1978 March 2

Summary. The extragalactic X-ray sources already identified are mainly active (Seyfert-type) galaxies or rich clusters. Using existing data, we discuss the possible outcome of the deeper surveys soon to be carried out with the next generation of X-ray telescopes. In particular, we use the quoted sensitivity of *HEAO-B* (for both point-like and resolved sources) to estimate how many sources of various kinds should be detectable in a given observing time. If the source population did not evolve with redshift, the X-ray source counts would be dominated by low-luminosity (10^{43}–10^{44} erg/s) clusters and Seyfert galaxies; a *HEAO-B* field, observed for 10^5 s, would have only a ~ 20 per cent chance of revealing a high-luminosity cluster with $z \simeq 2$. There is a greater likelihood of discovering remote clusters if they have evolved through a high-luminosity phase; and many (~ 10 per field) large-redshift point sources might be detected if the X-ray properties of quasars evolve at least as steeply as their optical properties. The existing evidence on small-scale isotropy excludes the possibility that rich clusters (however they have evolved) could contribute the whole X-ray background, and sets constraints on the contribution from quasars: if the background arises from discrete sources, they are mostly too faint to be detected individually by *HEAO-B*. General astrophysical arguments suggest that new categories of extragalactic X-ray sources – associated with (for instance) young galaxies or extended radio sources – may be discovered. We suggest how such objects might be recognized, emphasizing the importance of complementary programmes – e.g. deep radio surveys, objective prism plates, etc. – in an optimal observing strategy.

1 Introduction

The advent of imaging X-ray telescopes, such as the second High Energy Astronomy Observatory, *HEAO-B* (Giacconi & Schreier 1977a; see also Kellogg 1977), permits the possibility of a deep X-ray survey of the Universe. We indicate here what kind of extragalactic objects might be detectable by such a telescope and compare such observations with those made at other wavelengths. Kellogg (1977) has already predicted the appearance of the X-ray background from the *HEAO-B* detectors under the assumption that the low-energy ($E \lesssim 3$ keV) background is due to collapsing protoclusters of galaxies. We investigate this, and related hypotheses involving strong evolution of sources, together with the results to be expected from non-evolving populations of both clusters of galaxies, galactic nuclei and quasars. Accurate estimates of the number of unevolved sources allow evolved, or exotic, sources to be more readily recognized.

The *HEAO-B* X-ray observatory consists of four nested Wolter type-1 X-ray mirrors producing an image of size $\sim 1\frac{1}{4}°$ and resolution of a few arcseconds. Several different detectors may separately be used at the focal plane; we shall be concerned here with the Imaging Proportional Counter (IPC) of field 60×60 arcmin, resolution ~ 1 arcmin, and the High Resolution Imager (HRI) of field 25×25 arcmin, resolution ~ a few arcsec. Both operate over 0.2–0.3 and 0.5–4 keV. The efficiency of these devices is such that the IPC is the more sensitive to sources of dimension $\gtrsim 1$ arcmin, but the HRI rapidly becomes more sensitive to smaller sources. Further instrumental details are given by Giacconi & Schreier (1977a).

The limited lifetime of satellite instrumentation emphasizes the need for an optimum operational strategy. Later missions, such as the European X-ray Observing Satellite (*EXOSAT*) and the proposed next generation of larger telescopes, will benefit from, and add to, the data from *HEAO-B*.

2 The estimation of source counts

The number of sources per steradian brighter than S count/s has been estimated from

$$N(>S) = \int_{L_{\min}}^{L_{\max}} n(L, z=0)\, dL \int_0^{z(S)} \frac{[zq_0 + (q_0 - 1)(\sqrt{2q_0 z + 1} - 1)]^2}{q_0^4 (1+z)^3 (1 + 2q_0 z)^{1/2}}\, dz \tag{1}$$

(Weinberg 1972) where z and q_0 are the redshift and deceleration parameter respectively, and S is the observed X-ray count rate. The density of sources has been assumed not to evolve, and thus $n(L) = n(L, z=0)(1+z)^3$, where $n(L)$ is the luminosity function (comoving number density of sources with luminosities L to $L + dL$). The second integral was evaluated numerically for increments $\Delta z = z_2 - z_1$ at each of which $S(z_2)$ was obtained from

$$S(z) = \frac{LH_0^2 q_0^4 A \int_{E_1}^{E_2} E^{-1} \exp[-E(1+z)/T]\, dE}{1.7 \times 10^{-9}\, 4\pi c^2 T (zq_0 + (q_0 - 1)(\sqrt{2q_0 z + 1} - 1)^2} \tag{2}$$

where a bremsstrahlung spectrum of temperature T keV has been assumed and the effective detector area is A. The contributions for each Δz out to a chosen value of S were then summed to obtain $N(>S)$.

In practice the luminosity function was integrated at decade intervals, representing L by the mean luminosity for that interval. Δz was taken as 0.1. The *Uhuru* detectors were assumed to have $E_1 = 2$ keV, $E_2 = 6$ keV and $A = 1000\ \text{cm}^2$. This produced good agreement (within ~0.1) between predicted and observed count rates. The *HEAO-B* detectors were approximated by (1) IPC with $E_1 = 0.2$, $E_2 = 0.3$ keV, and further $E_1 = 0.5$, $E_2 = 3$ keV, both passbands with $A = 100\ \text{cm}^2$; and (2) HRI with similar energy bands, but the first with $A = 20\ \text{cm}^2$, the second with $A = 30\ \text{cm}^2$. These predicted counting rates that were within 10 per cent of those quoted in Giacconi & Schreier (1977a) for $T = 10$ keV.

A sensitivity limit of 5σ above detector background (taken to be 10^{-3} count arcmin^{-1} s^{-1}) was imposed, this being a reasonable statistical approach to the situation when $\sim 60^2$ pixels are searched for significant signals. (A pixel is taken to be 1 arcmin square.) We assume, of course, that the mean detector background is constant across the detector. The soft X-ray background is <0.5 times that of the detector background, but may vary across the field of view.

The sensitivity of photon-counting devices is such that the minimum detectable flux, $S_{\min}$, is inversely proportional to observing time t, until a few background photons are detected per pixel in t. Increasing the observing time when background limited gives $S_{\min} \propto t^{-1/2}$. The break point occurs at $t_b \simeq 10^4$ s for the IPC (1 arcmin pixel) and $\sim 10^6$ s for the HRI (6 arcsec pixel). Provided that cosmology is not affecting the source counts, and that $N\ (>S_{\min}) \propto S_{\min}^{-3/2}$, then the number of sources detected varies as $t^{3/2}(t < t_b)$ and $t^{3/4}(t > t_b)$. The maximum number of sources are observed in a given time interval if it is divided into as many samples of length t_b as possible.

2.1 CLUSTERS OF GALAXIES WITH NO LUMINOSITY EVOLUTION

Approximately one-third of the high-latitude ($|b| > 10^\circ$) X-ray sources found by current X-ray detectors have been identified as clusters of galaxies (2A catalogue: Cooke *et al.* 1978; 4U catalogue: Forman *et al.* 1978). Most of these sources are close to the limit of detectability, and are then subject to confusion errors (Warwick & Pye 1978), making the inferred luminosities uncertain by a factor up to ~ 2. Estimating the luminosity function of clusters by the volume ratio, V/V_m, method (Schmidt 1968) is consequently an unreliable process, but attempts to fit a power law (Rowan-Robinson & Fabian 1975; Schwartz 1978) are in rough agreement:

$$n(L)\,dL_{44} = (2 \pm 1) \times 10^5 L_{44}^{-2.3\pm0.3}(c/H_0)^{-3} \tag{3}$$

where L_{44} is the X-ray luminosity in units of 10^{44} erg/s.

The luminosity function may also be estimated by simulation of the X-ray source counts, together with knowledge of the extent to which various luminosity classes contribute. The wide distance range ($\gtrsim \times 10$) of the identified cluster X-ray sources (Bahcall 1977; Jones & Forman 1978), compared with the narrow flux interval ($\sim \times 2$) within which they are detected, indicates that the luminosity function has a slope ~ 2.5 in the observed range. The identifications are only reasonably complete out to a distance class $D = 3$ ($z \simeq 0.063$). Clusters with X-ray luminosities between $\sim 10^{44}$ and 10^{46} erg/s are well sampled in this volume, but any less or more luminous are undersampled. With the present data, it appears that the 10^{44-45} and 10^{45-46} erg/s classes contribute roughly equal numbers to the source counts above 2 *Uhuru* count/s. We have simulated the source counts to be expected, subject to this last constraint, from a range of power-law luminosity functions from equations (1) and (2). The best fit

$$n(L)\,dL_{44} = 1.7 \times 10^5\, L_{44}^{-2.5}(c/H_0)^{-3} \tag{4}$$

will be used henceforth. The cluster counts so produced constitute 50 per cent of the observed counts and are shown in Fig. 1 with the contributions of each decade of luminosity above 10^{43} erg/s. The 10^{43-44} erg/s contribution should be reduced by ~ 0.5, for it introduces a density of X-ray clusters greater than that of rich clusters, but, as the selection effects make this class uncertain, we treat it as an upper limit. It is not necessary to invoke a high-luminosity cut-off to (4). Cosmological effects become serious before the high-luminosity classes are able to contribute significantly to the source counts. The observed high-latitude

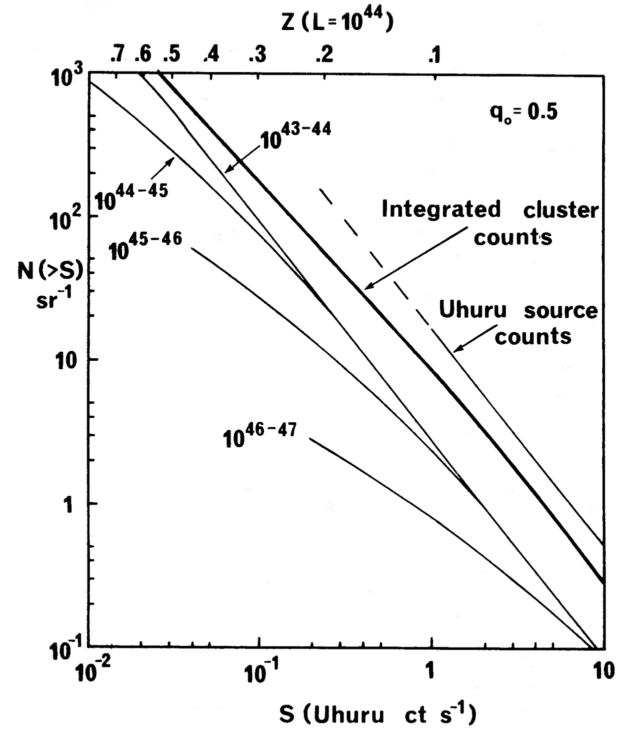

Figure 1. Integrated *Uhuru* source counts for unevolved clusters of galaxies of luminosity function equation (4). Contributions from various luminosity classes, in erg/s, are indicated, as well as the z at which a source of 10^{44} erg/s yields the corresponding *Uhuru* flux. Active galaxies produce a similar result, with additional contributions from sources weaker than 10^{43} erg/s.

X-ray source counts currently extend down to ~ 1 *Uhuru* count/s ($\equiv 1.7 \times 10^{-11}$ erg s^{-1} cm^{-2} (2–6 keV)) according to

$$N(>S)\, dS \simeq 17 S^{-3/2}\, dS/\mathrm{sr} \tag{5}$$

(Murray 1978; Warwick & Pye 1978), and are inferred to continue similarly down to ~ 0.2 *Uhuru* count/s from the background fluctuations (Fabian 1975; Warwick & Pye 1978).

The source counts resulting from applying the luminosity function (4) to the IPC and HRI of *HEAO-B* are indicated in Figs 2(a,b) and 3. The IPC source counts are shown for observing times of 10^5 and 10^6 s, and the HRI for 10^5 s only. The redshift range and corresponding *Uhuru* flux for clusters at the 5σ limit are shown in Table 1.

The major cluster contributor to each observation is the lowest luminosity class, which is the most uncertain. Approximately one cluster in the 10^{44}–10^{45} erg/s class is detected in 10^5 s with the IPC, at $z \simeq 0.8$. About six fields are required before there is a reasonable chance of observing a more luminous cluster at $z \simeq 2$. Changing q_0 from 0.5 to 0.05 makes little difference to the integrated counts. Increasing the observing time to 10^6 s allows the distant ($z \gtrsim 1.3$), 10^{44-45} erg/s, clusters to be studied, rather than merely detected, but the chance of obtaining a more luminous cluster in the field is still <0.25. It is clear that 10 separate 10^5 s fields yield more clusters than one 10^6 s field. The mean HRI field is devoid of detectable clusters, owing to their relative low surface-brightness (a radius of 250 kpc is assumed). This permits the HRI to be used as a means for discriminating between clusters and point sources. Since the IPC and HRI observations are made separately, variability of compact sources must be taken into account.

We have assumed throughout that the X-ray spectrum is that due to thermal bremsstrahlung at $kT = 10$ keV. Redshift reduces the effect of any soft X-ray enhancement from

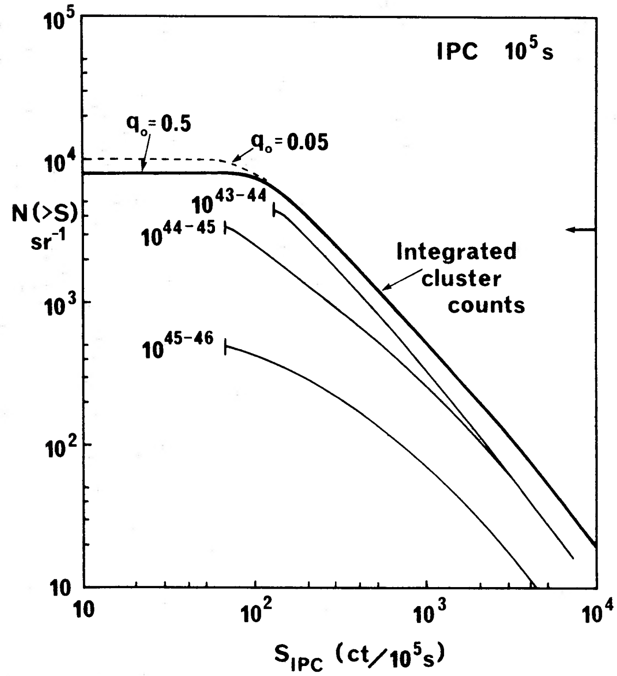

Figure 2. (a) Integrated IPC counts for clusters of galaxies for 10^5 s observing time. The effect of varying q_0 from 0.5 to 0.05 is shown. The arrow indicates the level at which one source occurs per square degree. A pixel size of 1 arcmin^2 has been assumed. Active galaxies give a similar result unless their spectra are steep or show significant absorption.

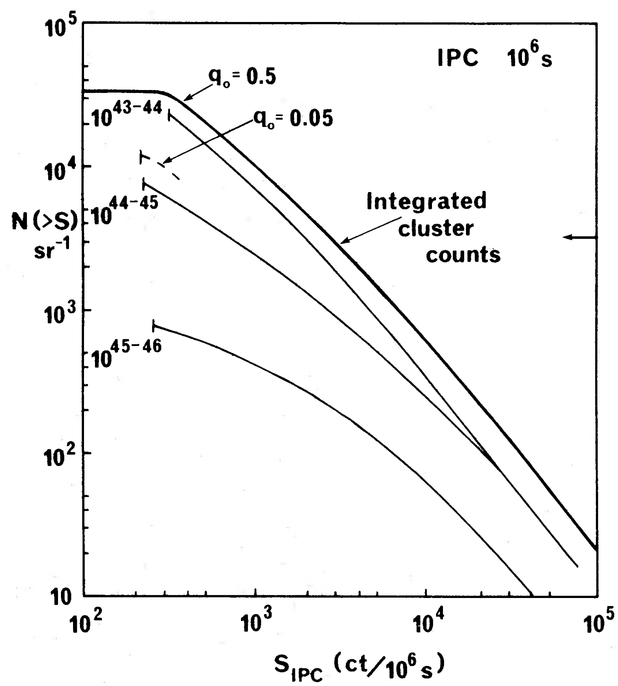

Figure 2. (b) Similar to Fig. 2(a) except that an observing time of 10^6 s has been used.

the clusters. A more realistic, but as yet unknown, temperature distribution for X-ray clusters may reduce the *HEAO-B* source counts by a factor ~ 2. A weakly increasing X-ray luminosity of clusters with decreasing redshift, such as suggested by Cowie & Perrenod (1978), would further reduce the *HEAO-B* source counts, especially of the more distant luminous sources.

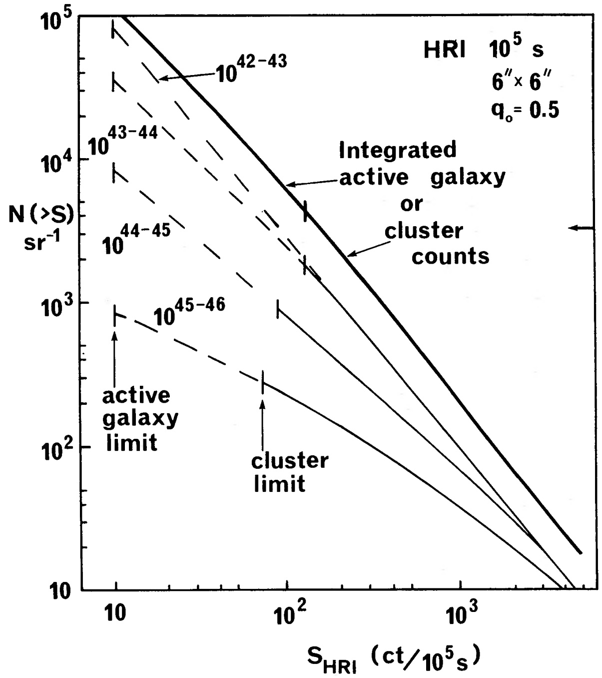

Figure 3. Integrated counts in the HRI after 10^5s at a pixel size of 6 × 6 arcsec. The extended size of clusters makes them unobservable below a higher flux level than active galaxies. The source counts above $S \simeq 100$ count/10^5s are reasonably reliable for clusters, and are roughly doubled by the addition of active galaxies if the spectra of these galaxies are similar to those of clusters over the 0.2–4 keV range. Active galaxies then dominate below $S \sim 100$ count/s with contributions as shown by the dashed lines.

A rough luminosity estimate of the clusters may be obtained if an approximately constant source-size can be assumed. The 10^{43-44} erg/s class becomes undetectable in the IPC in 10^5 s when they subtend a total angular size of ~ 2 arcmin (R = 250 kpc). High luminosity classes fall below the sensitivity level at a size of ~ 1 arcmin. Consequently a source occupying a single 1-arcmin pixel in the IPC and undetected in the HRI is mostly likely to be a cluster of luminosity exceeding ~ 10^{44} erg/s and $z > 0.3$.

2.2 CLUSTERS OF GALAXIES WITH STRONG LUMINOSITY EVOLUTION

Various authors (Doroshkevich, Sunyaev & Zel'dovich 1974; Gull & Northover 1975; Cavaliere & Setti 1976; Lea 1976; Maraschi & Perola 1975; Hartquist 1977; Cavaliere, Danese & De Zotti 1977; Kellogg 1977) have considered the cooling of protocluster gas at redshifts $z \simeq 2$–3. In general they have assumed these gas clouds to have an abrupt density falloff beyond some radius and that the temperature of the gas is the virial temperature for that mass of gas. We estimate here the source counts from the type of gas clouds that might be associated with Abell clusters (Fig. 4). We assume particle densities, n, up to that of the binding density of cluster cores ($n_c \simeq 0.2\,\mathrm{cm}^{-3}$), of size $R_c \simeq 250$ kpc. The temperature is assumed to be either the virial temperature for such a core, $T_v \simeq 10^8$K, or the free-fall temperature into a core, $T_{ff} \simeq 10^9$K.

One major problem with an initial phase of high luminosity due to strong cooling in clusters of galaxies is its compatibility with their low present luminosities. The luminosity can only diminish sufficiently rapidly between $z = 2$ and 0 if there is little hot gas beyond the core, implying that cluster formation left much less than 1 per cent of the total cluster mass as gas. A more extended atmosphere would still be cooling now, generating high

Table 1. Clusters (R = 250 kpc) in IPC, $q_0 = 0.5$.

L	t	S_{IPC}	z_{IPC}	S_{Uhuru}	θ
2.5×10^{43}	10^5	158	0.2	5.9×10^{-3}	0.99
	10^6	36	0.4	1.3×10^{-3}	0.65
2.5×10^{44}	10^5	77	0.8	2.5×10^{-3}	0.58
	10^6	25	1.3	7.2×10^{-4}	0.48
2.5×10^{45}	10^5	79	2.1	1.9×10^{-3}	0.51
	10^6	27	3.2	5.2×10^{-4}	0.59
2.5×10^{46}	10^5	<154	>4.0	$<2.4 \times 10^{-3}$	>0.65
Clusters (R = 250 kpc) in IPC, $q_0 = 0.05$.					
2.5×10^{43}	10^5	144	0.2	5.4×10^{-2}	0.94
	10^6	30	0.4	1.1×10^{-3}	0.59
2.5×10^{44}	10^5	76	0.7	2.5×10^{-3}	0.45
	10^6	18	1.2	5.4×10^{-4}	0.37
2.5×10^{45}	10^5	56	1.8	1.4×10^{-3}	0.35
	10^6	18	2.6	3.9×10^{-4}	0.34
2.5×10^{46}	10^5	52	3.8	8.6×10^{-4}	0.34
Point source in HRI, $q_0 = 0.5$.					
2.5×10^{42}	10^5	28	0.1	2.6×10^{-3}	
	10^6	7	0.2	5.9×10^{-4}	
2.5×10^{43}	10^5	15	0.4	1.3×10^{-3}	
	10^6	4	0.7	3.5×10^{-4}	
2.5×10^{44}	10^5	10	1.3	7.2×10^{-4}	
	10^6	4	2.1	2.2×10^{-4}	
2.5×10^{45}	10^5	10	3.3	4.7×10^{-4}	
	10^6	<6	>4.0	2.4×10^{-4}	

Notes:

(1) $L, t, S_{\mathrm{IPC}}, S_{Uhuru}$ and θ are in erg/s, s, count, count/s and arcmin respectively.
(2) Values are taken to the largest z in intervals $\Delta z = 0.1$.
(3) Evolutionary effects almost certainly invalidate estimates for $z > 1$.
(4) Quantization of θ in measurement owing to discrete pixel size increases the above flux estimates.

luminosities. We have parametrized our uncertainty in luminosity fall-off as a power-law decrease,

$$L = L_0(t/t_c)^{-\alpha} \quad (t > t_c) \tag{6}$$

where t_c is the initial cooling time. We assume that cooling commences at $z = 3$ ($q_0 = ½$). Various α between 10 and 2 are required, depending upon L_0 and t_c.

Strong cooling and consequent high luminosities may also be terminated if sufficient heat is put into the gas that an outflow is created (*cf.* Yahil & Ostriker 1973). Quasars, supernovae and other explosive events may be involved. Accretion of the cooling gas could perhaps trigger off, or generate, such activity.

The spectrum and isotropy of the X-ray background provide a further constraint on possible high-luminosity phases of source evolution. Representative *HEAO-B* source counts are shown in Fig. 4 for three possible cases in terms of the number density of clusters, N_H per 'Hubble volume' $(c/H_0)^3$, temperature T, α and particle density n. The integrated

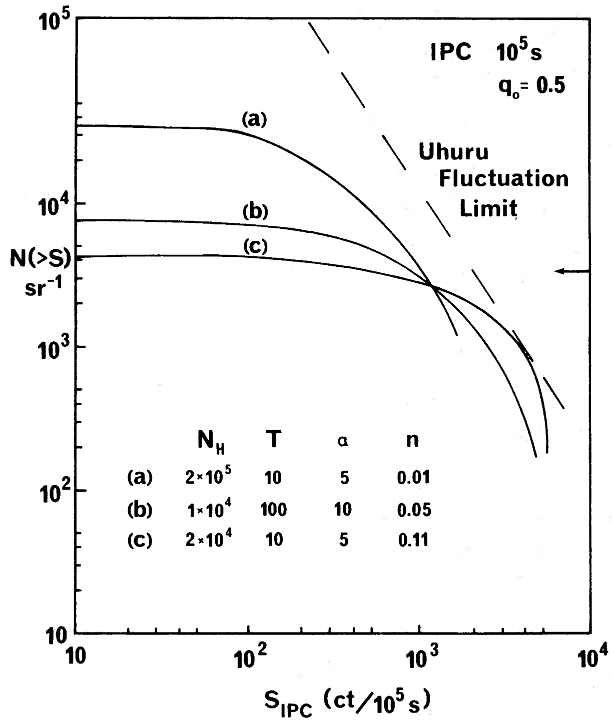

Figure 4. Integrated counts due to three models of evolved clusters of galaxies. N_H, T, α and n are the number of sources per $(c/H_0)^3$, temperature, luminosity decay parameter and particle density. The sources are 250 kpc in radius and cool from $z = 3$. For the fluctuation limit see Fig. 5.

X-ray background in these cases is <0.1 of that observed; the spatial fluctuations in the background prove to be the tightest constraint.

All of the observed *Uhuru* fluctuations are attributable to sources just below the detectability threshold (Fabian 1975). We estimate that evolved sources contribute fluctuations of amplitude $\lesssim 1$ per cent in the *Uhuru* 5 x 5° field of view. This restricts

$$N(>S) \lesssim 3.8 S^{-2}\, \mathrm{sr}^{-1} \quad (S < 0.1) \tag{7}$$

in *Uhuru* count/s. This limit is shown in Fig. 5, and transferred to Fig. 4 for the *HEAO-B* detectors. Equation (7) is likely to be overestimated unless the emission from protoclusters is extended by $\gtrsim 10$ Mpc. The production of the entire integrated background intensity requires, at most

$$N(>S) \simeq 2.2 \times 10^3 S^{-1}\, \mathrm{sr}^{-1}, \tag{8}$$

the precise relationship depending upon the overall shape of the source counts (as does equation (7)).

Rich clusters of galaxies, of maximum density $4 \times 10^5 (c/H_0)^{-3}$ (Rowan-Robinson 1970) yield, within $z = 3$, less than 1.2×10^5 or 3×10^5 sources sr^{-1} if $q_0 = 0.5$ or 0.05 respectively. These limits are shown in Fig. 5 and demonstrate that rich clusters can contribute at most 30 or 50 per cent of the X-ray background. Clusters produce unacceptable fluctuations if these values are exceeded. Even at these limits some special form of evolution is required. Less rich clusters than Abell class 0, or groups, may be invoked but it is not clear that sufficiently high temperatures can then be obtained to match the spectrum of the observed background. (They could, however, feature at low energies in *HEAO-B* samples.)

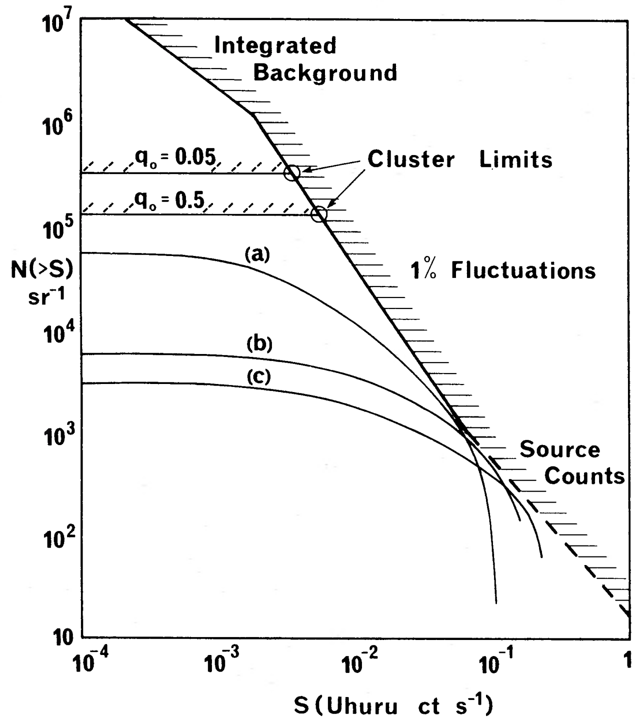

Figure 5. Integrated background and fluctuation constraints plotted in *Uhuru* units. Both constraints depend in detail upon the form of the actual source counts. Three evolving protocluster cases are shown as in Fig. 4. The total surface density obtainable from $z \leqslant 3$ for rich clusters of number density $4 \times 10^5 (c/H_0)^{-3}$ is indicated for $q_0 = 0.5$ and 0.05. It is clear that rich clusters cannot reach the integrated background line without contradicting the fluctuation constraint.

Rich clusters may provide an important contribution to the 20–50 keV background if a significant luminosity is emitted at T_{ff}. The dynamics and consequences of both the $T = T_{\text{v}}$ and $T = T_{\text{ff}}$ cases are discussed more fully by Fabian & Nulsen (in preparation).

We conclude this section by noting that high luminosities from clusters of galaxies at redshifts $z = 1$–3 may have occurred, but require additional hypotheses. These are (1) that effectively *all* the gas has cooled, (2) that cooling occurred during a transient dynamic phase, or that (3) cooling was terminated by violent events followed by an outflow. Fig. 4 depicts a reasonable upper limit to be expected from events related to cluster formation that is compatible with observed clusters at the current epoch, and observation of the X-ray background.

2.3 ACTIVE GALAXIES AND QUASARS

The active galaxies (mostly Seyfert galaxies) identified with high-latitude X-ray sources are similar to rich clusters in number and distance range, which strongly suggests that these two classes of objects have similar X-ray luminosity functions. This is borne out by estimates based on the V/V_{m} test (Elvis *et al.* 1978; Tananbaum *et al.* 1978). We have therefore adopted equation (4) as being the X-ray luminosity function of active galaxies also. The source counts of active galaxies are then identical to those of the clusters, excepting for the surface-brightness cut-off. This is of little consequence in the IPC, as both distant clusters and active galaxies occupy only one pixel. Strong differentiation does, however, occur in the HRI, and we have extended these counts down to the sensitivity limit of a 6×6 arcsec pixel (Fig. 3).

There is no need to impose a cut-off to the active galaxy luminosity function at a value as high as $\sim 10^{43}$ erg/s, and consequently it is likely that low-luminosity active galaxies may dominate the source counts in both detectors. There are several caveats to this, however:

(a) Photoelectric absorption within the active galaxy may severely reduce the low-energy X-ray emission (*cf.* Cen-A, Stark, Davison & Culhane 1976; NGC 4151, Barr *et al.* 1977). This becomes less important for galaxies at significant redshifts. IPC spectra are important in assessing this problem.

(b) Strong evolution may be important. The current (highly uncertain) quasar X-ray identifications are compatible with the 10^{46}–10^{47} erg/s class in the *Uhuru* source counts (Fig. 1). It is possible that quasars represent the high-luminosity tail of the luminosity function. Counts of optically observed quasars (Setti & Woltjer 1973) indicate that the integral counts follow a slope of -1.5. If a similar slope may be applied to the X-ray counts then it is unlikely that quasars dominate the *HEAO-B* source counts. At best they might contribute a similar number to the 10^{42-43} erg/s class in Fig. 3, but that requires most of the, as yet, unidentified, sources above 1 *Uhuru* count/s to be quasars. The presence of more than one quasar per square degree implies, from the quasar counts of Setti & Woltjer, that the -1.5 slope persists at magnitudes fainter than $B \simeq 18$.

Since most of these quasars have $z \gtrsim 1$, a -1.5 slope implies a drastic evolutionary effect on the comoving density of optically luminous quasars. It is, of course, possible that the X-ray properties of quasars evolve differently, so that the distribution of L_X/L_{opt} is itself epoch-dependent. The fluctuation constaint in Fig. 5 still applies, however. *HEAO-B* observations should settle this question (as well as augmenting the very scanty existing data on the X-ray luminosity function of quasars).

3 Other classes of extragalactic X-ray sources

The available data on the X-ray properties of clusters and active galactic nuclei, though limited, give us confidence that the quantitative extrapolations in Section 2 are worthwhile. *HEAO-B* may, however, reveal *new* categories of cosmologically-interesting X-ray sources, and we mention two such possibilities here. Our discussion is brief because we are guided only by order of magnitude estimates.

3.1 COMPTON SCATTERING IN REMOTE RADIO SOURCES

Inverse Compton scattering of microwave background photons by relativistic electrons was long ago suggested as a contributor to the X-ray background (Felten & Morrison 1966). This process would tend to be more efficient at large redshifts, for two reasons (*cf.* Bergamini, Londrillo & Setti 1969; Felten & Rees 1969): the energy density of the microwave background varies as $(1+z)^4$; and the many suppliers of relativistic electrons – radio source, quasars, etc. – were more prolific at early epochs. As a corollary of this effect, Compton scattering may 'snuff out' extended sources at large redshifts (Rees & Setti 1968; Rowan-Robinson 1970; Scheuer 1977).

X-rays observed in the range 1–10 keV are generated predominantly by electrons with Lorentz factors in the range $(1–3) \times 10^3$. The radio sources with the highest inverse Compton X-ray luminosities are therefore those with the largest energy content in the form of such electrons. These sources will not necessarily be those with the highest radio luminosities: the maximum stored energy is inferred to exist in very extended 'giant' sources and in the low surface-brightness 'bridges' joining the components of some strong double sources. On the assumption of equipartition, the energy stored in relativistic electrons in NGC 6251 and 3C 236 is $\gtrsim 10^{60}$ erg (Waggett, Warner & Baldwin 1977; Willis, Strom & Wilson 1974): and the energy is indeed mainly in electrons with γ of $\sim 10^3$, these being the values corresponding to the low-frequency end of the radio (synchrotron) spectrum. If the magnetic field is weaker than its equipartition strength, the inferred energy stored in relativistic electrons is even larger.

A radio source with a typical spectral index ~ 0.7 containing $10^{60}\epsilon_{60}$ erg of relativistic electrons with $\gamma \gtrsim 10^3$, and at redshift z, will emit an inverse Compton X-ray power of $\sim 3 \times 10^{43}(1+z)^4\epsilon_{60}$ erg/s. We do not know the appropriate values of ϵ_{60}, but it would seem quite probable that there may be diffuse objects at $z \simeq 2$, a few hundred kpc in extent, emitting $\sim 10^{46}$ erg of 1–10 keV X-rays. These sources would generally *not* be particularly powerful radio sources (objects such as Cygnus A or 3C 9 are powerful radio sources because they have a strong magnetic field, rather than because they have an exceptional energy content), but they may feature in deep radio surveys.

3.2 YOUNG GALAXIES

According to some theories, galaxies pass through a bright early phase when the rate of star formation, supernova outbursts, etc., is $\gtrsim 100$ times higher than in a present-day galaxy (Ostriker & Thuan 1975; Meier 1976). The properties of such systems, and their potential detectability, depend on many uncertainties; but we can readily see that a young galaxy where supernova outbursts were frequent could give rise to thermal X-rays with a *hard* spectrum.

A supernova ejects debris at speeds $\sim 10^4$ km/s. When the ejecta from separate supernovae collide, shocks raise the kinetic temperature to $\sim 10^9$ K ($\sim$ 100 keV). This hot material would be expelled from the galaxy as a wind, provided that radiative cooling is unimportant on the outflow time-scale. Further shock-heating would occur when the winds from individual 'young galaxies' in a cluster interacted. This process would generate a patchy distribution of thermal X-rays with a spectrum characterized by temperatures exceeding T_V. (This scenario would provide a way of halting the infall into a cluster and thereby terminating the bright phase discussed in Section 2.2.) It also, of course, suggests how the intergalactic gas in clusters could have been contaminated by heavy elements (*cf.* Mitchell *et al.* 1976).

3.3 THE X-RAY BACKGROUND

The discussion in Section 2.2 shows that rich clusters of galaxies cannot alone produce the 2–6 keV X-ray background, even with evolution. Any candidate sources for the background must, from the constraints in Fig. 5, be more numerous than $\sim 10^6\,\mathrm{sr}^{-1}$ and weaker than $\sim 2 \times 10^{-3}$ *Uhuru* count/s. The *HEAO-B* detectors are just capable of detecting any sources at this limit in 10^5 s, although there would then be $\sim$ 500 per field if they constituted the X-ray background. Extrapolations of existing source counts, such as the -1.5 quasar slope discussed in Section 2.3, might give the background at $\sim 6 \times 10^{-5}$ *Uhuru* count/s, but this requires $\sim 10^4$ quasars per square degree. (The rather less quantifiable processes described earlier could also contribute, as indeed could several rather more speculative processes occurring at large redshifts.) *HEAO-B* may clarify the various contributions of different types of sources, but is unlikely to image the X-ray background completely.

The present discussion suggests that the 2–6 keV X-ray background may not all be due to point-like sources. A total number of sources $\gtrsim 1$ per cent of that of all galaxies is required, unless they are all at $z \gg 1$. We conjecture, however, that at energies >10 keV inaccessible to *HEAO-B* the main contributors may be active nuclei and quasars (which appear to have hard spectra), extended radio galaxies at large redshifts and possibly very hot gas in clusters. These considerations suggest that it is important to improve limits on, and estimates of, fluctuations in both 2–6 keV and > 10 keV X-ray backgrounds. If the relative contributions of different source populations depend on energy, it is unlikely that the X-ray background spectrum is smooth and featureless.

4 An observing strategy, and complementary programmes

Ten (or more) separate samples with the IPC of 10^5 s observing time each, such as suggested in the *HEAO-B* consortium observing programme (Giacconi & Schreier 1977b), with HRI images of the same fields, should reveal a significant number of clusters of galaxies (~10–20) and active galaxies or quasars (<100). The majority of these objects will be at small redshifts ($z \lesssim 0.5$): although a few will appear at $z \simeq 1$. Spending more time on each field does not increase the number of distant clusters in proportion to the investment in observing time. Clusters may be studied in some detail, but it would seem more advantageous to spend that time studying the much brighter clusters found by previous scanning instruments.

Objective prism surveys, followed by detailed optical study, are important in obtaining cluster and active galaxy redshifts. Clusters of galaxies evolving through a high-luminosity phase may be detected in some of the *HEAO-B* fields. Optical recognition of these events may prove fruitless, but a search for microwave dips (Sunyaev & Zel'dovich 1972) may be worthwhile:

$$\frac{\Delta T}{T} = 2\tau_{es}\left(\frac{kT_e}{m_e c^2}\right),$$

so a particle density of $\sim 0.1\,\mathrm{cm^{-3}}$ in the core of a cluster implies an electron scattering optical depth $\tau_{es} \simeq 0.05$. $\Delta T/T$ is thus ~ 0.02 if $T = T_{ff}$, or ~ 0.002 if $T = T_V$. Such a core subtends ~1 arcmin at $z \simeq 2$–3 and thus fills about one-quarter of the beam of a 60-m dish operated at 3 cm. Dips of 5×10^{-2} to 5×10^{-3} are thus expected and may have been detected (Cavaliere *et al.* 1977; Lake & Partridge 1977; Gull & Northover 1976). Failure to observe the predicted dips might indicate that the emitting gas was patchy (*cf.* Section 3.2). Alternatively, extended X-ray emission detected in the IPC without variation, and yet not in the HRI, may be due to inverse Compton radiation in radio lobes. A sensitive radio map of the region can test this.

It may, indeed, be worthwhile selecting some regions containing known interesting objects that extend over a limited region of the field of view. In this way the deep survey can be extended whilst also completing other observing programmes that require 10^{4-5} s of IPC observing time. HRI observations of all such fields, not necessarily of 10^5 s, may subsequently permit discrimination between clusters and active galaxies.

If photoelectric absorption within active galaxies is not a problem, most of those objects should be at $z \lesssim 0.4$ and discernible on optical Sky Survey plates. Only if there are active galaxies in which L_X/L_{opt} greatly exceeds that in known sources can no immediate optical candidate be expected.

On the basis of present information we expect the following possibilities:

(1) Sources extended over several IPC pixels are probably clusters of galaxies with $z \lesssim 0.2$. This could be checked on optical Sky Survey plates.

(2) A source detected in one IPC pixel but not in an HRI 6-arcsec pixel, with no evidence for variability, could be one of the following:

(a) If there were no associated microwave dip, nor a single radio source at the same position, it would probably be a more distant cluster with $z \lesssim 1$. Optical techniques (*cf.* Gunn & Oke 1975) may confirm this.

(b) If a microwave dip were present, it would be most likely a protocluster (see Sections 2.2 and 3.2). A patchy distribution may be expected in the HRI, especially since any protoclusters detected may be well above the sensitivity limit.

(c) If a single radio source (perhaps itself extended) were observed, the X-rays could then result from the inverse Compton mechanism (see Section 3.1). An estimate of magnetic field is then possible.

(3) Any sources observed in the HRI 6-arcsec pixels are expected to be observed in the IPC unless they are weak or variable:

(a) If there were an associated galaxy on optical Sky Survey plates, it would probably be an active galaxy with $z \lesssim 0.4$.

(b) An optical counterpart that appeared stellar with emission lines would be a quasar, radio emission then being possible.

(c) No optical candidate indicates exceptional L_X/L_{opt}. (We have throughout assumed that the samples are taken at high galactic latitudes such that interstellar reddening and X-ray absorption in our Galaxy can be neglected.)

5 Conclusions

Present data are sufficient to estimate the unevolved population of X-ray sources expected in a typical deep X-ray survey. The most numerous sources (up to 10 per square degree in 10^5 s of *HEAO-B* observing time) have small redshifts ($z \lesssim 0.2$) and are likely to be active galaxies. To detect the greatest number of sources, it is best to observe as many samples as possible that are *just* background limited. Longer observing times increase the depth of the survey by *less* than $t^{1/4}$, as cosmology becomes important. A *HEAO-B* observing time of 10^5 s gives a reasonable chance of observing a few clusters out to $z \simeq 1$.

Categories of evolved sources, such as quasars and protoclusters, that may contribute significantly to the X-ray background have been considered. It seems unlikely that more than 10 such sources occur per square degree. Observations of clusters of galaxies at the present epoch, together with X-ray background observations, limit the extent to which clusters may have passed through a very luminous phase. A surface density $\gtrsim 10^6$ source/sr is needed to produce the 2–6 keV X-ray background. It is therefore unlikely that the main contribution comes from rich clusters, or indeed from sources individually resolved by *HEAO-B*. Complementary optical, radio and microwave studies are necessary in order to identify candidate objects for X-ray sources found in deep surveys.

Acknowledgments

We are indebted to Professor Giacconi and his colleagues at the Center for Astrophysics for preprints containing quantitative information about *HEAO-B* on which some of our calculations have been based. ACF acknowledges a Radcliffe Fellowship. We gratefully acknowledge early collaboration with Professor G. Setti.

References

Bahcall, N. A., 1977. *Astrophys. J.*, **217**, L77.
Barr, P., White, N. E., Sanford, P. W. & Ives, J. C., 1977. *Mon. Not. R. astr. Soc.*, **181**, 43P.
Bergamini, R., Londrillo, P. & Setti, G., 1969. *Nuovo Ciuvento*, **52B**, 495.
Cavaliere, A. & Setti, G., 1976. *Astr. Astrophys.*, **46**, 81.
Cavaliere, A., Danese, L. & De Zotti, G., 1977. *Astrophys. J.*, **217**, 6.

Cooke, B. A., Ricketts, M. J., Maccacaro, T., Pye, J. D., Elvis, M., Watson, M. G., Griffiths, R. E., Pounds, K. A., McHardy, I., Maccagni, D., Seward, F. D., Page, C. G. & Turner, M. J. L., 1978. *Mon. Not. R. astr. Soc.*, **182**, 489.
Cowie, L. L. & Perrenod, S. C., 1978. *Astrophys. J.*, **219**, 354.
Doroshkevich, A. G., Sunyaev, R. A. & Zel'dovich, Y. B., 1974. In *Confrontation of cosmological theory with observations*, ed. Longair, M. S., D. Reidel, Dordrecht, Holland.
Elvis, M., Maccacaro, T., Wilson, A. S., Ward, M. J., Penston, M. V., Fosbury, R. A. E. & Perola, G. C., 1978. *Mon. Not. R. astr. Soc.*, **183**, 129.
Fabian, A. C., 1975. *Mon. Not. R. astr. Soc.*, **172**, 149.
Felten, J. E. & Morrison, P., 1966. *Astrophys. J.*, **146**, 686.
Felten, J. E. & Rees, M. J., 1969. *Nature*, **221**, 924.
Forman, W., Jones, C., Cominsky, L., Julien, P., Murray, S., Peters, G., Tananbaum, H. & Giacconi, R., 1978. *Astrophys. J. Suppl.*, in press.
Giacconi, R. & Schreier, E. J., 1977a. *Center for Astrophysics document*, HEA-76-143.
Giacconi, R. & Schreier, E. J., 1977b. *Center for Astrophysics document*, *HEAO-B* Consortium Observing Programme.
Gull, S. F. & Northover, K. J. E., 1975. *Mon. Not. R. astr. Soc.*, **173**, 585.
Gull, S. F. & Northover, K. J. E., 1976. *Nature*, **263**, 572.
Gunn, J. E. & Oke, J. B., 1975. *Astrophys. J.*, **195**, 255.
Hartquist, T. W., 1977. *Astrophys. J.*, **217**, 3.
Jones, C. & Forman, W., 1978. *Astrophys. J.*, in press.
Kellogg, E., 1977. *Astrophys. J.*, **218**, 582.
Lake, G. & Partridge, R. B., 1977. *Nature*, **270**, 502.
Lea, S. M., 1976. *Astrophys. J.*, **203**, 569.
Maraschi, L. & Perola, G. C., 1975. *Astr. Astrophys.*, **40**, 387.
Meier, D., 1976. *Astrophys. J.*, **207**, 343.
Mitchell, R. J., Culhane, J. L., Davison, P. J. N. & Ives, J. C., 1976. *Mon. Not. R. astr. Soc.*, **176**, 29P.
Murray, S., 1978. *Astrophys. J.*, in press.
Ostriker, J. P. & Thuan, T. X., 1975. *Astrophys. J.*, **202**, 353.
Rees, M. J. & Setti, G., 1968. *Nature*, **217**, 326.
Rowan-Robinson, M., 1970. *Mon. Not. R. astr. Soc.*, **150**, 389.
Rowan-Robinson, M. & Fabian, A. C., 1975. *Mon. Not. R. astr. Soc.*, **170**, 199.
Scheuer, P. A. G., 1977. In *Radio astronomy and cosmology*, p. 343, ed. Jauncey, D., D. Reidel, Dordrecht, Holland.
Schmidt, M., 1968. *Astrophys. J.*, **151**, 393.
Schwartz, D. A., 1978. *Astrophys. J.*, **220**, 8.
Setti, G. & Woltjer, L., 1973. Sixth Texas symposium on relativistic astrophysics, ed. Hegyi, D. J., *Ann. N.Y. Acad. Sci.*, **224**, 8.
Stark, J. P., Davison, P. J. N. & Culhane, J. L., 1976. *Mon. Not. R. astr. Soc.*, **174**, 35P.
Sunyaev, R. A. & Zel'dovich, Y. B., 1972. *Comm. Astrophys. Sp. Phys.*, **4**, 173.
Tananbaum, H., Peters, G., Forman, W., Giacconi, R., Jones, C. & Avni, Y., 1978. *Astrophys. J.*, in press.
Waggett, P. C., Warner, P. J. & Baldwin, J. E., 1977. *Mon. Not. R. astr. Soc.*, **81**, 465.
Warwick, R. S. & Pye, J. P., 1978. *Mon. Not. R. astr. Soc.*, **183**, 169.
Weinberg, S., 1972. *Gravitation and cosmology*, Wiley, New York.
Willis, A. G., Strom, R. G. & Wilson, A. S., 1974. *Nature*, **250**, 625.
Yahil, A. & Ostriker, J. P., 1973. *Astrophys. J.*, **185**, 787.

Note added in proof

Calibration data (F. D. Seward, private communication) indicate that the *HEAO-B* HRI is not as sensitive as we have assumed. The HRI sensitivity to point sources is now similar to that of the IPC.

Mon. Not. R. astr. Soc. (1978) **185**, 123–135

Frequency dependence of radio-source counts and spectral index distributions

V. K. Kulkarni *Tata Institute of Fundamental Research, Homi Bhabha Road, Colaba, Bombay 400005, India*

Received 1978 March 7; in original form 1977 November 22

Summary. The problem of predicting radio-source counts at different frequencies, and the related problem of calculating the expected variations in spectral index distributions with flux density, are discussed in terms of evolutionary world models. It is shown that, by using different forms of cosmological evolution for flat- and steep-spectrum radio sources and by including the correlation between radio luminosity and spectral index, the existing models can be modified to produce source counts and spectral index distributions which agree better with those observed both at 408 MHz and 5 GHz than do the distributions predicted by earlier models.

1 Introduction

The problem of relating the spectral index distributions of radio sources at different frequencies and in different flux density ranges has been discussed by many authors (Kellermann, Pauliny-Toth & Davis 1968; van der Laan 1969; Fanaroff & Longair 1973; Petrosian & Dickey 1973). It has become apparent that in order to explain recent data it may be necessary to modify these models. This paper describes calculations of the expected variations of the spectral index distributions with flux density and frequency for evolutionary cosmological models. The possibility that the cosmological evolution can be different for flat- and steep-spectrum sources has been considered, together with the known correlation between radio luminosity and spectral index. An attempt has been made to derive a generalized luminosity function $\psi(P, z, \alpha)$. This generalized luminosity function (GLF) describes the comoving space density of extragalactic radio sources as a function of radio luminosity P (measured in $\mathrm{WHz^{-1}\,Sr^{-1}}$), redshift z and spectral index α. The GLF is chosen to give source counts and spectral index distributions consistent with observational data from surveys at 408 MHz and 5 GHz.

Section 2 points out some of the assumptions made in the earlier models and the difficulties these models encounter in view of the recent data on source counts and spectral index distributions at 5 GHz. The details of the present model and procedure are described in Section 3. The predictions of different models are then compared with the observations in Section 4. It is shown that the data are consistent with an evolutionary model in which radio luminosity and spectral index are correlated and in which the densities of flat- and steep-spectrum sources evolve in different ways.

In this paper, the spectral index α is defined by the relation $S \propto \nu^{-\alpha}$; radio sources with $\alpha < 0.5$ are called flat-spectrum sources and those with $\alpha > 0.5$ are called steep-spectrum sources.

2 Earlier models

In the past, essentially two approaches have been taken in relating source counts at different frequencies to a known spectral index distribution at one frequency. In the first, described by Kellermann, Pauliny-Toth & Davis (1968) and van der Laan (1969), it is assumed that the spectral index distribution is independent of flux density at one frequency. The source counts and spectral index distributions at another frequency are then calculated by convolving the source counts with the known distributions. The high- and low-frequency source counts are found to be in reasonable agreement, but this formalism is unsatisfactory for two reasons. The first is the assumption that the spectral index distribution is independent of flux density at some frequency and the second is the neglect of the detailed information present in the source counts regarding differential cosmological evolution of radio sources in widely different luminosity ranges.

Fanaroff & Longair (1973) (see also Petrosian & Dickey 1973; Schmidt 1972) have given a more general and satisfactory formalism. They estimated the spectral index distributions and source counts from models of space distributions of radio sources, i.e. from the GLF $\psi(P, z, \alpha)$, and found the predicted variation of spectral index distributions at high frequencies to be in fairly good agreement with the observations. However, Pauliny-Toth (1977) has pointed out that this model predicts consistently lower source counts at 5 GHz for the weak sources, a discrepancy which reaches a factor of about 3 at ~ 0.02 Jy, the limiting flux density of the deep surveys. This agreement has also been noted by Davis & Taubes (1974) in their $P(D)$ analysis of data from the NRAO 5-GHz deep survey by Davis (1971).

Davis (1977) has measured spectral indices between 1.4 and 4.8 GHz for a sample of weak radio sources selected at 4.8 GHz. In a sample of 61 sources with flux densities > 0.009 Jy at 4.8 GHz, 34 per cent of the sources have flat spectra ($\alpha < 0.5$). The fraction of flat-spectrum sources is essentially unchanged (36 per cent) for sources with flux densities > 0.02 Jy. On the other hand, the model by Fanaroff & Longair predicts a value of ~ 18 per cent for the fraction of flat-spectrum sources at these very small flux densities.

In their model, Fanaroff & Longair also made the following assumptions for the sake of simplicity:

(1) The form of evolution is identical for sources with flat and steep spectra. However, in the last few years many authors have suggested differences in the evolution of flat- and steep-spectrum quasars (Rowan-Robinson 1972, 1976; Setti & Woltjer 1973; Fanti *et al.* 1975). Recently, for example, Schmidt (1976) has analysed a sample of 51 quasars from the NRAO 5-GHz survey, using the V/V_m test. The three subsamples $\alpha > 0.45$, $0.45 > \alpha > 0.05$ and $\alpha < 0.05$, each of which contains 17 objects, yield values for $\langle V/V_m \rangle$ of 0.71 ± 0.05, 0.60 ± 0.07 and 0.52 ± 0.06 respectively, indicating that there are indeed differences in the evolution of these subsamples. From a study of a complete sample selected at 2700 MHz, Masson & Wall (1977) reached similar conclusions. They used spectral indices which are virtually identical to two-point 2.7 –5.0-GHz spectral indices, and found values $\langle V/V_m \rangle = 0.52 \pm 0.05$ for a subsample of 42 flat-spectrum quasars with $\alpha < 0.5$ and 0.67 ± 0.05 for a subsample of 15 steep-spectrum quasars. From these results, alorg with the source counts

and the relation between evolution and radio structure (Rowan-Robinson 1972), Masson & Wall (1977) suggested that the cosmological evolution of both quasars and galaxies is confined to the powerful sources with extended structure. Since a majority of the powerful extended sources have steep spectra, this implies that in general the evolution of sources with steep spectra is stronger than that of flat-spectrum sources.

Furthermore, the source counts expressed as n/n_0 have a broader maximum at high frequencies than at low frequencies (Fomalont, Bridle & Davis 1974; Wall & Cooke 1975). The range in flux density over which this maximum occurs corresponds to some luminosity range $\Delta P = P_2 - P_1$ (Longair 1971). The cosmological evolution is confined to those sources which have their luminosity in the range P_1 to P_2. Thus the broader maximum of source counts at high frequencies implies that this range ΔP is larger. Also, at high frequencies the contribution to the source counts from flat-spectrum sources is comparatively large. Hence it is natural to assume that this range ΔP is larger for flat-spectrum sources.

We have given above only the simplest explanation of the broader maximum in the high-frequency counts. The truth is probably much more complex. For instance, ΔP may be epoch-dependent, and in different ways for flat- and steep-spectrum sources, or ΔP may be the same width but centred differently for flat- and steep-spectrum sources. Both these effects also give rise to broader maxima at high frequencies. However, these factors are not included in the present model because they would make it more complex, with added free parameters.

(2) The spectral index function $n(\alpha)$ and the luminosity function $\rho(P, z)$ are independent at a low frequency. This is equivalent to factorizing the GLF $\psi(P, z, \alpha)$ in the form

$$\psi(P, z, \alpha) = \rho(P, z) n(\alpha). \tag{1}$$

A correlation between radio luminosity P and spectral index α for sources selected at 178 MHz has, however, been reported by many authors (Kellermann, Pauliny-Toth & Williams 1969; Bridle, Kesteven & Guindon 1972; Macleod & Doherty 1972; Véron, Véron & Witzel 1972). It appears that this correlation is statistically significant for a class of radio sources consisting mostly of radio galaxies with spectral indices $\alpha > 0.5$.

These above possibilities have been taken into account in modifying the model of Fanaroff & Longair.

3 The present model

3.1 GENERAL FORMALISM

Let us assume that there are two classes of sources. Most of the steep-spectrum sources for which radio luminosity and spectral index are correlated form one class. The remainder are the flat-spectrum sources for which radio luminosity and spectral index are not correlated. The GLF $\psi(P, z, \alpha)$ can then be written in the following form

$$\psi(P, z, \alpha) = \rho(P, z = 0)\,[C_f F_f(P, z) n_f(\alpha) + C_s F_s(P, z) n_s(\alpha\,|\,P)] \tag{2}$$

where

$\rho(P, z = 0)$ = local luminosity function
C_f = fraction of flat-spectrum sources
C_s = fraction of steep-spectrum sources
$F_f(P, z)$ = evolution function for flat-spectrum sources
$F_s(P, z)$ = evolution function for steep-spectrum sources
$n_f(\alpha)$ = normalized spectral index function for the flat-spectrum radio sources
$n_s(\alpha\,|\,P)$ = normalized spectral index function (i.e. the conditional probability distribution) for the steep-spectrum sources for a given luminosity P.

A suitable form for $n_f(\alpha)$ and $n_s(\alpha|P)$ needs to be chosen. Petrosian & Dickey (1973) have shown that a bimodal spectral index function consisting of two Gaussians, one centred around $\alpha = 0.4$ and another around $\alpha = 0.8$ gives good agreement at 408 MHz. In view of this we have chosen the following forms:

$$n_f(\alpha) = \frac{1}{\sigma_f\sqrt{2\pi}} \exp\left[-(\alpha - \alpha_{0f})^2/2\sigma_f^2\right] \tag{3}$$

and

$$n_s(\alpha|P) = \frac{1}{\sigma_s\sqrt{2\pi}} \exp\left[-(\alpha - \alpha_{0s})^2/2\sigma_s^2\right] \tag{4}$$

where σ_f, σ_s and α_{0f} are treated as free parameters. In general α_{0s} is a function of luminosity. The correlation between P and α is introduced in the formalism through α_{0s}. A larger value of P would imply a larger value of α_{0s} around which $n_s(\alpha|P)$ will be centred. If α_{0s} is independent of luminosity P, then $n_s(\alpha|P) = n_s(\alpha)$ will be independent of luminosity P. However, in general both α_{0s} and σ_s are functions of radio luminosity. With a view to keeping the model as simple as possible but still including dependence of spectral index function on luminosity, we have considered the luminosity dependence of α_{0s} only. In any case, as pointed out by Fanaroff & Longair (1973) and Petrosian & Dickey (1973), these correlations are not likely to make any appreciable changes in the results. A relation between α_{0s} and P was obtained by using the relation

$$\int \alpha n_s(\alpha|P) d\alpha = \langle\alpha\rangle = \alpha_{0s}(P). \tag{5}$$

Hence one needs to calculate the mean value of spectral index for sources in different luminosity ranges. For this we took a sample of 96 sources consisting of all the identified radio sources with $S_{408} > 10$ Jy (Grueff & Vigotti 1977). For these sources, two-point spectral indices between 408 MHz and 5 GHz are available. We divided the sources into 12 luminosity bins, each bin containing eight sources. (Luminosities were calculated in an Einstein–de Sitter model for which $q_0 = ½$ and cosmological constant $\Lambda = 0$. A value of 50 km s^{-1} Mpc^{-1} was used for the Hubble constant H_0.) From each bin, sources with $\alpha < 0.6$ were removed and averages $\langle\log P\rangle$ and $\langle\alpha\rangle$ were calculated. From a plot of $\langle\alpha\rangle$ versus $\langle\log P\rangle$ (Fig. 1) it is seen that $\langle\log P\rangle$ and $\langle\alpha\rangle$ are correlated. A straight line fitted by least-squares is given by

$$\alpha_{0s} = \langle\alpha\rangle = -0.14 + 0.04\,\langle\log P\rangle. \tag{6}$$

As mentioned above, many authors have noted a correlation between radio luminosity and spectral index. Most of these authors have used spectral indices over a range of frequencies, whereas we have used two-point spectral indices. Also these authors obtain lines fitted by least-squares without pre-averaging the data, in contrast to our procedure. Moreover they considered specific classes of objects for studying this effect, for example, elliptical radio galaxies (Véron *et al.* 1972). For these reasons the relation for α_{0s} given above cannot be directly compared with those by others.

3.2 THE CHOICE OF WORLD MODEL AND LUMINOSITY FUNCTION

We have considered only the Einstein–de Sitter model in our calculations because the geometric differences between various world models are small in comparison with the effects

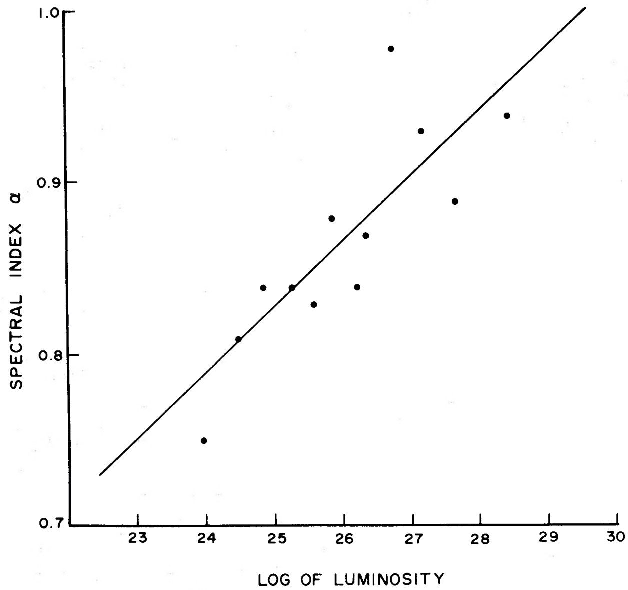

Figure 1. Plot of average spectral index ⟨α⟩ for each luminosity bin against log of luminosity (expressed in $\mathrm{WHz^{-1}\,Sr^{-1}}$).

of evolution. The local luminosity function and the evolution function for the steep-spectrum sources were taken to be those in model 4b by Wall, Pearson & Longair (1977). We have used this model because Wall *et al.* (1977) seem to prefer it after comparing redshift distributions predicted by different models with the identifications for the 5C3 survey. Moreover, this model is shown to produce angular size counts of extragalactic radio sources, which are in agreement with the observational data (Subrahmanya 1977). We have assumed the same local luminosity function for flat- and steep-spectrum sources, because with the data available at present it is not possible to derive the local luminosity function for flat-spectrum sources. No systematic optimizing procedure for deriving model parameters has been followed since we only wish to demonstrate that the incorporation of some observed effects into source-count models leads to consistency for counts and spectral index distributions at 408 MHz and 5 GHz.

3.3 THE CALCULATIONS

In the Einstein–de Sitter model the redshift $z(P, S, \alpha)$ up to which a radio source of spectral index α and luminosity $P(\nu)$ at the frequency of observation ν (ν being 408 MHz in our case) can have a flux density greater than the limiting flux density $S(\nu)$, is the solution of

$$P(\nu) = \frac{4c^2}{H_0^2} S(\nu)\,[1-(1+z)^{-1/2}]^2(1+z)^{1+\alpha} \tag{7}$$

The number of sources with spectral indexes in the range α and $\alpha + d\alpha$; luminosities in the range P and $P + dP$ and the volume bounded by $z(P, S, \alpha)$ is

$$\int_0^{z(P,S,\alpha)} \psi(P, z, \alpha)\frac{dV(z)}{dz} dz\, d\alpha\, dP \tag{8}$$

where dV is the comoving volume element.

The number of sources with flux density $\geqslant S$ and with spectral indexes in the range α and $\alpha + d\alpha$ is

$$dN(>S, \alpha)d\alpha = \int_{P(\nu)} dP \int_0^{z(P,S,\alpha)} \psi(P, z, \alpha) \frac{dV(z)}{dz} dz\, d\alpha. \tag{9}$$

The spectral index distribution at frequency ν is then given by

$$^{S}f_{\nu}(\alpha) = \frac{dN(>S, \alpha)}{\int_{\alpha} dN(>S, \alpha)\, d\alpha}, \tag{10}$$

and the source counts at frequency ν by

$$N(>S) = \int_{\alpha} dN(>S, \alpha)\, d\alpha. \tag{11}$$

The formalism can be modified to calculate the source counts and spectral index distributions at some other frequency in the following way. Let $^{S'}f_{\nu'}(\alpha)$ be the spectral index distribution for all the sources whose flux density $\geqslant S'$ at frequency ν' (= 5 GHz in the present case), and let $N'(>S')$ be the number of sources with flux density $\geqslant S'$ at ν'. Now a source with luminosity P at frequency ν will have a luminosity P' at frequency ν', given by

$$P' = P(\nu/\nu')^{\alpha}. \tag{12}$$

Using this relation for P', equations similar to (10) and (11) can be obtained for $^{S'}f_{\nu'}(\alpha)$ and $N'(>S')$.

3.4 THE MODELS

We have considered three models A, B and C depending on whether radio luminosity P and spectral index α are correlated or not and on whether flat- and steep-spectrum sources differ in their density evolution.

3.4.1 Model A

In this model P and α are correlated. The evolution of flat-spectrum sources is different from the evolution of steep-spectrum sources. We then assume that

$$\psi(P, z, \alpha) = \rho(P, z = 0)[C_f F_f(P, z) n_f(\alpha) + C_s F_s(P, z) n_s(\alpha | P)] \tag{13}$$

where

$$F_f(P, z) = \exp\,[M_f(P)(1 - t/t_0)]; \quad t = \frac{2(1+z)^{-1.5}}{3H_0}, \quad t_0 = \text{present epoch},$$

with

$$M_f(P) = 0 \quad \text{for } \log P < \log P_{f1} = 22.5;$$

$$M_f(P) = M_{f\,\max} = 8.0 \quad \text{for } \log P > \log P_{f2} = 28.0;$$

$$M_f(P) = M_{f\,\max} \frac{(\log P - \log P_{f1})}{(\log P_{f2} - \log P_{f1})} \quad \text{for } \log P_{f1} < \log P < \log P_{f2};$$

$$F_f(P, z) = 0 \quad \text{if } z > z_c = 3.5;$$

and

$$F_s(P, z) = \exp\,[M_s(P)(1 - t/t_0)],$$

with

$M_s(P) = 0 \quad$ for $\log P < \log P_{s1} = 25.0$;

$M_s(P) = M_{s\,max} = 11.0 \quad$ for $\log P > \log P_{s2} = 27.3$;

$$M_s(P) = M_{s\,max}\frac{(\log P - \log P_{s1})}{(\log P_{s2} - \log P_{s1})} \quad \text{for } \log P_{s1} < \log P < \log P_{s2};$$

$F_s(P, z) = 0 \quad$ if $z > z_c = 3.5$

and

$C_f = 0.05, \quad C_s = 0.95,$

$$n_f(\alpha) = \frac{1}{\sigma_f\sqrt{2\pi}}\exp\,[-(\alpha - \alpha_{0f})^2/2\sigma_f^2], \quad \text{with } \sigma_f = 0.25, \quad \alpha_{0f} = 0.25,$$

and

$$n_s(\alpha\,|\,P) = \frac{1}{\sigma_s\sqrt{2\pi}}\exp\,[-(\alpha - \alpha_{0s})^2/2\sigma_s^2], \quad \text{with } \sigma_s = 0.20,$$

$$\alpha_{0s} = -0.14 + 0.04\,\langle \log P\rangle.$$

3.4.2 *Model B*

In this model both flat- and steep-spectrum sources evolve in the same manner. P and α are correlated.

$$\psi(P, z, \alpha) = \rho(P, z = 0)\,F(P, z)[C_f n_f(\alpha) + C_s n_s(\alpha\,|\,P)], \tag{14}$$

where

$F(P, z)$ = same as $F_s(P, z)$ in model A,

$C_f = 0.015, \quad C_s = 0.985.$

All other parameters are the same as in model A.

3.4.3 *Model C*

In this model, flat- and steep-spectrum sources evolve in the same manner and P and α are assumed to be independent.

$$\psi(P, z, \alpha) = \rho(P, z = 0)\,F(P, z)\,[C_f n_f(\alpha) + C_s n_s(\alpha\,|\,P) \tag{15}$$

with $\alpha_{0s} = 0.83$. All other parameters are the same as in model B above. In essence, model C is that of Fanaroff & Longair.

In all these models the ratio C_f/C_s seems to indicate a remarkably low proportion of flat-spectrum objects, considering that such objects constitute more than 50 per cent of the 5-GHz count and ~ 10 per cent of the 408-MHz count. This can be explained in the following way.

5

Table 1. Comparison of predicted and observed spectral index distributions at 408 MHz.

Reference for observations	Flux density S at 408 MHz (Jy)	Frequencies (MHz)	Median spectral index α_{med}				Fraction of flat-spectrum sources $f_\alpha \leqslant 0.5$			
			Observed	Model A	Model B	Model C	Observed	Model A	Model B	Model C
Pauliny-Toth &	$S > 11.8$	408–5000	0.75 ± 0.02	0.81	0.82	0.78	0.10	0.09	0.08	0.10
Kellermann (1972a)	$11.8 > S > 8.7$	408–5000	0.80 ± 0.03	0.81	0.82	0.77	0.06	0.09	0.08	0.11
	$8.7 > S > 6.9$	408–5000	0.83 ± 0.03	0.81	0.82	0.76	0.10	0.09	0.08	0.12
	$6.8 > S > 4.1$	408–5000	0.83 ± 0.03	0.81	0.81	0.76	0.06	0.09	0.09	0.12
	$4.0 > S > 2.21$	408–5000	0.82 ± 0.03	0.81	0.81	0.75	0.15	0.09	0.09	0.13
	$2.19 > S > 0.89$	408–5000	0.83 ± 0.02	0.80	0.80	0.75	0.10	0.09	0.09	0.13
	$0.86 > S > 0.48$	408–5000	0.78 ± 0.03	0.81	0.81	0.76	0.13	0.10	0.09	0.12
	$0.4 > S > 0.2$	408–5000		0.80	0.80	0.76		0.10	0.07	0.10
	$0.1 > S > 0.05$	408–5000		0.76	0.79	0.78		0.15	0.08	0.08
	$0.05 > S > 0.02$	408–5000		0.75	0.79	0.81		0.22	0.10	0.08

For a given luminosity class at 408 MHz, sources with small α (flat-spectrum) can be observed to larger redshift at a given flux density than those with large α. In the above models, the comoving space density of sources increases rapidly with redshift. This increases the fraction of flat-spectrum sources in the 408-MHz sample to ~ 10 per cent. In the high-frequency sample (5 GHz), this fraction is further enhanced by the induced strong correlation between small α (flat-spectrum) and high radio luminosity at 5 GHz. This is one of the main points of the model introduced by Fanaroff & Longair (1973).

4 The results

4.1 THE SOURCE COUNTS AND SPECTRAL INDEX DISTRIBUTIONS AT 408 MHz

For each of the three models mentioned, the parameters were obtained by trial and error by requiring that the calculated source counts and the spectral index distributions be consistent with the observations at 408 MHz and 5 GHz. The spectral index distributions at 408 MHz are compared with those observed (Pauliny-Toth & Kellermann 1972a) in Table 1. For each model we have calculated the fraction of flat-spectrum sources ($\alpha < 0.5$) and the median value of spectral index α_{med} in different flux density ranges. All three models give fairly good agreement with the observational results. However, there are two differences in the predictions by different models. Firstly, model A predicts an increase in the fraction of flat-spectrum sources with decreasing flux density at a flux density level of ~ 0.05 Jy at 408 MHz. It is interesting to note that, from a study of spectral indices between 408 and 1400 MHz, Katgert (1975) has reported a marginally significant increase in the fraction of flat-spectrum sources below about 0.06 Jy at 408 MHz. A quantitative comparison is not very meaningful because of the different types of spectral indices involved and different ways of classifying sources as having flat- and steep-spectra. Secondly, at high flux densities models A and B predict a larger value for the median spectral index than does model C. This is expected, because in models A and B we have considered the correlation between P and α. The increase in α with decreasing flux density observed by Murdoch (1976) at 408 MHz is not predicted by any of these models. However, these predictions cannot be directly compared with Murdoch's result since the observations refer to two-point spectral indices between 408 MHz and 2.7 GHz whereas, in models A, B and C, two-point spectral indices between 408 MHz and 5 GHz are used. The extension of the present work to predict source counts and spectral index distributions at 1400 MHz and 2.7 GHz, by using the relevant two-point spectral index distributions, is in progress.

We started with a model, i.e. model 4b of Wall *et al.* (1977), which predicts source counts at 408 MHz in very good agreement with those observed. The model was derived by assuming a spectral index of 0.75 for all the sources. We have modified this model by introducing a spectral index distribution and different form of cosmological evolution for flat- and steep-spectrum sources. Hence models A, B and C give source counts different from those predicted by the model 4b mentioned above. Among the models A, B and C the best agreement between predicted and observed source counts is obtained with model A. In Fig. 2 we compare the normalized differential source counts predicted by model A with the observed source counts (Wall *et al.* 1977) and the agreement between the two is seen to be reasonably good.

4.2 THE SPECTRAL INDEX DISTRIBUTIONS AND SOURCE COUNTS AT 5 GHz

The predicted spectral index distributions are compared with those observed (Pauliny-Toth & Kellermann 1972b; Condon & Jauncey 1974; Davis 1977) in Table 2. In this table we have

Table 2. Comparison of predicted and observed spectral index distributions at 5000 MHz.

References for observations	Flux density S at 5000 MHz (Jy)	Frequencies (MHz)	Median spectral index α_{med}				Median spectral index $\alpha_{n\,med}$ for sources with $\alpha > 0.5$				Fraction of flat-spectrum sources $f_\alpha \leqslant 0.5$			
			Observed	Model A	Model B	Model C	Observed	Model A	Model B	Model C	Observed	Model A	Model B	Model C
Pauliny-Toth & Kellermann (1972b)	$S \geqslant 1.5$	408–5000	0.30 ± 0.06	0.36	0.34	0.39		0.70	0.70	0.67	0.57 ± 0.10	0.60	0.61	0.61
	$1.5 > S \geqslant 1.0$	408–5000	0.35 ± 0.05	0.41	0.45	0.45		0.70	0.70	0.67	0.60 ± 0.09	0.57	0.55	0.56
	$1.0 > S \geqslant 0.8$	408–5000	0.54 ± 0.06	0.44	0.49	0.48		0.70	0.70	0.67	0.47 ± 0.09	0.56	0.51	0.53
	$0.8 > S \geqslant 0.6$	408–5000	0.55 ± 0.05	0.46	0.51	0.51		0.70	0.70	0.67	0.45 ± 0.07	0.54	0.47	0.49
	$0.6 > S \geqslant 0.1$	408–5000	0.60 ± 0.07	0.56	0.64	0.60		0.72	0.72	0.69	0.43 ± 0.10	0.43	0.28	0.32
	$0.1 > S \geqslant 0.067$	408–5000	0.63 ± 0.04	0.60	0.68	0.65		0.73	0.73	0.70	0.40 ± 0.09	0.38	0.20	0.22
Condon & Jauncey (1974)	$S > 1.15$	318–5000	0.34 ± 0.15	0.38	0.38	0.41	*0.66 ± 0.027	0.70	0.70	0.67	0.56 ± 0.05	0.59	0.59	0.59
	$1.15 > S \geqslant 0.8$	318–5000	0.43 ± 0.07	0.43	0.48	0.48	0.73 ± 0.03	0.70	0.70	0.67	0.57 ± 0.05	0.56	0.52	0.53
	$0.8 > S \geqslant 0.6$	318–5000	$0.55^{+0.04}_{-0.11}$	0.46	0.51	0.51	0.70 ± 0.024	0.70	0.70	0.67	0.48 ± 0.05	0.54	0.47	0.49
	$0.6 > S \geqslant 0.25$	318–5000	$0.49^{+0.10}_{-0.15}$	0.51	0.59	0.56	0.79 ± 0.05	0.71	0.71	0.67	0.52 ± 0.08	0.49	0.37	0.41
	$0.25 > S \geqslant 0.067$	318–5000	$0.57^{+0.02}_{-0.03}$	0.59	0.67	0.63	0.76 ± 0.021	0.73	0.73	0.70	0.43 ± 0.04	0.40	0.23	0.26
Davis (1977)	$S > 0.02$	1400–5000	0.60	0.62	0.71	0.73		0.76	0.76	0.68	0.36	0.38	0.18	0.20
	$S > 0.009$	1400–5000		0.62	0.72	0.74		0.76	0.77	0.70	0.34	0.39	0.17	0.16

* Condon & Jauncey (1974) have estimated the median value of spectral index $\alpha_{n\,med}$ by a slightly different procedure which involves passing the distribution through a mathematical window of width ~0.4. The median value is chosen in such a way that the median coincides with the window centre.

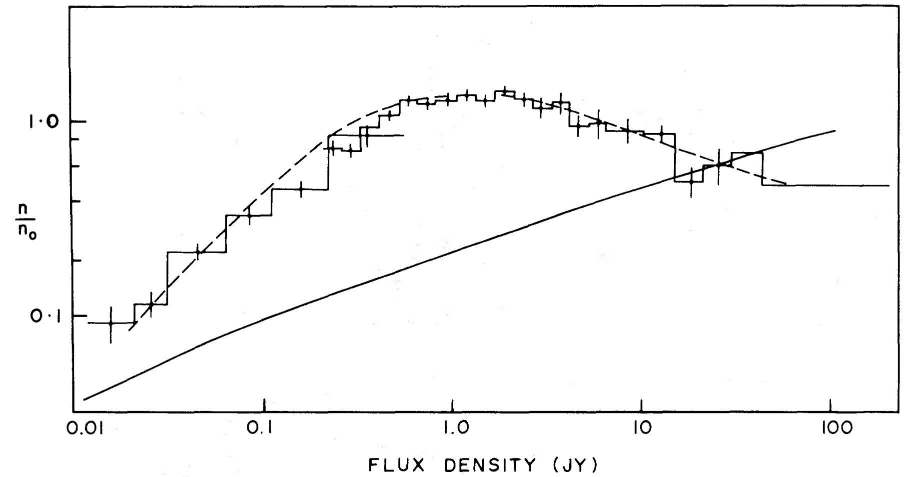

Figure 2. The normalized differential source counts at 408 MHz. The observed counts are taken from Wall *et al.* (1977). The solid curve is for a non-evolutionary, source-converging model; the dashed curve is for model A.

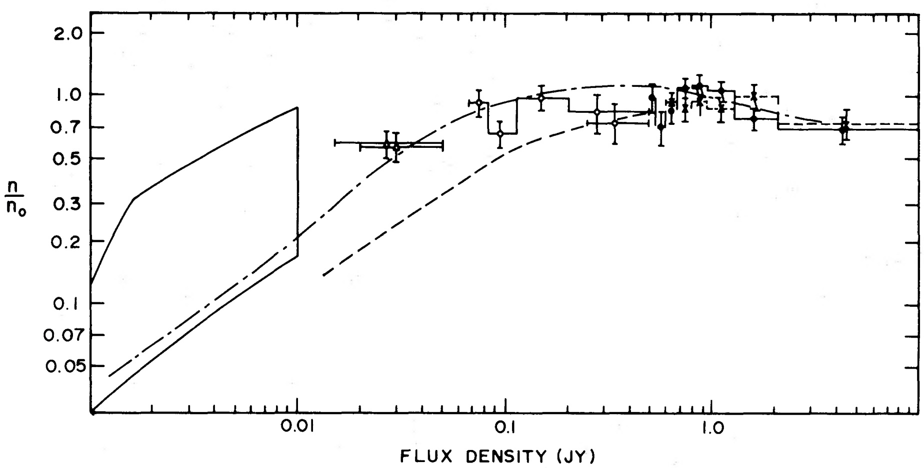

Figure 3. The normalized differential source counts at 5 GHz. The observed counts are denoted as follows: • NRAO–MPIR(S); ○ NRAO(D); △ MPIR; × PARKES; and the area outlined in the lower left-hand corner represents limits (from background deflection analysis) on the number–flux density relation between 0.01 and 0.001 Jy (Pauliny-Toth 1977; Wall & Cooke 1975). The dashed curve (taken from Pauliny-Toth 1977) indicates predictions from the model by Fanaroff & Longair while the dot–dash curve corresponds to model A.

listed, for each model and in different flux density ranges, the fraction of sources with $\alpha < 0.5$, the median value (α_{med}) of the spectral index for the whole distribution, and the median spectral index ($\alpha_{\mathrm{n\,med}}$) for the steep-spectrum sources ($\alpha > 0.5$). At high and intermediate flux densities all the models are in agreement with the observational data, but at flux density levels below ~ 0.1 Jy, models B and C predict too low a value for the fraction of flat-spectrum sources. At these flux densities only model A is in agreement with the observational data. Moreover, model A produces a better agreement with the observed source counts at 5 GHz than do the other two models. The normalized differential source counts predicted by model A are compared in Fig. 3 with the observed source counts (Pauliny-Toth 1977), and those predicted by the model of Fanaroff & Longair. The agreement between the predicted counts (model A) and those observed is satisfactory. It is interesting to note that it is the different evolutions of flat- and steep-spectrum sources which produce the better agreement. The effect of inclusion of a P–α correlation is small.

However, as pointed out earlier, we have not followed any systematic optimizing procedure to obtain the best values of parameters for agreement with observations. Our main aim was to see whether by modifying the conventional models, it would be possible to produce better agreement with the source counts and spectral index distributions and we have shown that it is indeed possible to obtain models which are consistent with the observations. In view of the large number of free parameters involved, such models are in no way unique. Also we have assumed the same local luminosity function for both flat- and steep-spectrum sources, since an insufficient number of identified flat-spectrum sources is present in the low-frequency samples. When more data become available, the local luminosity function can be separately determined for flat- and steep-spectrum sources. At low frequencies the effect of using a separate local luminosity function for flat-spectrum sources is small, because of the small fraction of flat-spectrum sources involved. The parameters of the local luminosity function for flat-spectrum sources will give additional freedom and it may be possible to get better agreement between the model predictions and observational data at high frequencies.

The redshift distributions and identification at different flux levels place additional constraints on these models. The differences between models A, B, C and model 4b of Wall *et al.* (1977) are small as far as predictions at 408 MHz are concerned. Since model 4b is known to predict redshift distributions which are in agreement with the observational data, models A, B and C also predict correct redshift distributions. It is only at high frequencies (in the present case 5 GHz) that the differences between models become important. Hence, in order to narrow down the choice of models, observational data giving redshift distributions of sources selected at a high frequency become very important.

It may also be necessary to approach the problem in a more systematic way and carry out an optimizing procedure to obtain predictions which are in agreement with observations at many different frequencies.

5 Conclusions

We have derived a generalized luminosity function $\psi(P, z, \alpha)$ by incorporating into the conventional models the different forms of cosmological evolution for flat- and steep-spectrum radio sources and the correlation between radio luminosity and spectral index. This generalized luminosity function is shown to be consistent with the source counts and spectral index distributions at both 408 and 5000 MHz. It is shown that:

(1) the improvement over earlier models is due to the inclusion of different forms of cosmological evolution for flat- and steep-spectrum sources,

(2) the effect of incorporation of the correlation between radio luminosity and spectral index is small.

More observational data (especially for flat-spectrum sources) are needed to determine this generalized luminosity function better.

Acknowledgments

It is a pleasure to thank Professor T. K. Menon for suggesting the problem and for valuable discussions. I thank a referee for suggesting improvements in the presentation of this paper.

References

Bridle, A. H., Kesteven, M. J. L. & Guindon, B., 1972. *Astrophys. Lett.*, **11**, 27.
Condon, J. J. & Jauncey, D. L., 1974. *Astr. J.*, **79**, 1220.

Davis, M. M., 1971. *Astr. J.*, **76**, 980.

Davis, M. M., 1977. In IAU Symp. 74, *Radio astronomy and cosmology*, ed. Jauncey, D. L., D. Reidel, Dordrecht, Holland.

Davis, M. M. & Taubes, C., 1974. *Bull. Am. astr. Soc.*, **6**, 485.

Fanaroff, B. L. & Longair, M. S., 1973. *Mon. Not. R. astr. Soc.*, **161**, 393.

Fanti, C., Fanti, R., Ficarra, A., Formiggini, L., Giovanni, G., Lari, C. & Padrielli, L., 1975. *Astr. Astrophys.*, **42**, 365.

Fomalont, E. B., Bridle, A. H. & Davis, M. M., 1974. *Astr. Astrophys.*, **36**, 273.

Grueff, G. & Vigotti, M., 1977. *Astr. Astrophys.*, **54**, 475.

Katgert, P., 1975. *Astr. Astrophys.*, **49**, 221.

Kellermann, K. I., Pauliny-Toth, I. I. K. & Davis, M. M., 1968. *Astrophys. Lett.*, **2**, 105.

Kellermann, K. I., Pauliny-Toth, I. I. K. & Williams, P. J. S., 1969. *Astrophys. J.*, **157**, 1.

Longair, M. S., 1971. *Rep. Prog. Phys.*, **34**, 1125.

Macleod, J. M. & Doherty, L. H., 1972. *Nature*, **238**, 88.

Masson, C. R. & Wall, J. V., 1977. *Mon. Not. R. astr. Soc.*, **180**, 193.

Murdoch, H. S., 1976. *Mon. Not. R. astr. Soc.*, **177**, 441.

Pauliny-Toth, I. I. K., 1977. In IAU Symp. 74, *Radio astronomy and cosmology*, ed. Jauncey, D. L., D. Reidel, Dordrecht, Holland.

Pauliny-Toth, I. I. K. & Kellermann, K. I., 1972a. *Astr. J.*, **77**, 560.

Pauliny-Toth, I. I. K. & Kellermann, K. I., 1972b. *Astr. J.*, **77**, 797.

Petrosian, V. & Dickey, J., 1973. *Astrophys. J.*, **186**, 403.

Rowan-Robinson, M., 1972. *Nature*, **236**, 112.

Rowan-Robinson, M., 1976. *Nature*, **262**, 97.

Schmidt, M., 1972. *Astrophys. J.*, **176**, 303.

Schmidt, M., 1976. *Astrophys. J.*, **209**, L55.

Setti, G. & Woltjer, L., 1973. *Ann. N.Y. Acad. Sci.*, **224**, 8.

Subrahmanya, C. R., 1977. *PhD thesis*, University of Bombay.

van der Laan, H., 1969. *Bull. astr. Inst. Netherl.*, **20**, 171.

Véron, M. P., Véron, P. & Witzel, A., 1972. *Astr. Astrophys.*, **18**, 82.

Wall, J. V. & Cooke, D. J., 1975. *Mon. Not. R. astr. Soc.*, **171**, 9.

Wall, J. V., Pearson, T. J. & Longair, M. S., 1977. In IAU Symp. 74, *Radio astronomy and cosmology*, ed. Jauncey, D. L., D. Reidel, Dordrecht, Holland.